Defence Science Journal, Vol. 63, No. 2, March 2013, pp. 145-152, DOI: 10.14429/dsj.63.4256

REVIEW PAPER

Fusion of Onboard Sensors for Better Navigation

Ravi Shankar

Hindustan Aeronautics Limited, Hyderabad–500 042, India
E-mail: ravishankar0507@gmail.com

ABSTRACT

This paper presents simulation results of navigation sensors such as integrated navigation system (INS), global navigation satellite system (GNSS) and TACAN sensors onboard an aircraft to find the navigation solutions. Mathematical models for INS, GNSS (GPS) satellite trajectories, GPS receiver and TACAN characteristics are simulated in Matlab. The INS simulation generates the output for position, velocity and attitude based on aerosond dynamic model. The GPS constellation is generated based on the YUMA almanac data. The GPS dilution of precession (DOP) parameters are calculated and the best combination of four satellites (minimum PDOP) is used for calculating the user position and velocity. The INS, GNSS, and TACAN solutions are integrated through loosely coupled extended Kalman filter for calculating the optimum navigation solution. The work is starting stone for providing aircraft based augmentation system for required navigation performance in terms of availability, accuracy, continuity and integrity.

Keywords: Extended Kalman filter, multisensor data fusion, integrated navigation system, global navigation satellite system, GPS Constellation, GPS Receiver, TACAN

1. INTRODUCTION

Sensors onboard an aircraft are integrated navigation system (INS), global navigation satellite system (GNSS), TACAN, radio altimeter, surface radar tracker (ground proximity warning system), link 16, air data computer and forward looking sensors (LiDAR, RADAR, Visible/ IR) which assists pilot for navigation. However, it is extremely difficult for the pilot to rely on any one instrument and the decision making depends on pilot's proficiency. This study and simulation amalgamates outputs from these sensors and processes it through a navigation filter for providing best solutions for RNP in terms of availability, accuracy, integrity and continuity. The RNP parameters[1,2] and area navigation[3] are defined in literature. Many papers and books had discussed the integration of navigation sensors[4], Kalman filter (KF) for fusion of INS and GPS[5,6,] fusion of different sensors[5,7,] loosely coupled integration of GPS and INS using EKF[8], loose integration of INS, GPS and camera[9], INS and GPS on ultra tightly system[10-12]. However, in this paper various navigation sensors are simulated and the navigation data fusion problem is deeply examined with the aim of developing an EKF suitable for exploiting existing navigation sensors in various manned and unmanned aircraft for both civil and military applications.

INS provides standalone solution. Long duration solution from INS is achieved by using very high quality accelerometers and gyros which increase the cost of navigation system. GNSS navigation solution depends on the availability of GNSS signals which in turn is dependent upon numerous factors such as location, antenna orientation and dilution of precision (DOP). TACAN is used by military for range and bearing with respect to TACAN ground station.

The scope of multi sensor data fusion is shown in Fig. 1. The EKF is selected as a prime data fusion method to provide navigation solution.

2 SENSOR MODELS

The sensor models such as INS, GNSS constellation, GNSS receiver and TACAN are required. The GNSS receiver works in the earth centre earth fix (ECEF) coordinate system. The other sensors provide solutions in a local coordinate frame.

The INS is simulated by simulating the accelerometers, gyros, bias, scale factor and white noise random drift. The generalised mathematical model which are used in simulation for gyros, accelerometer and derive velocity, acceleration, position (errors) are described in Appendix I.

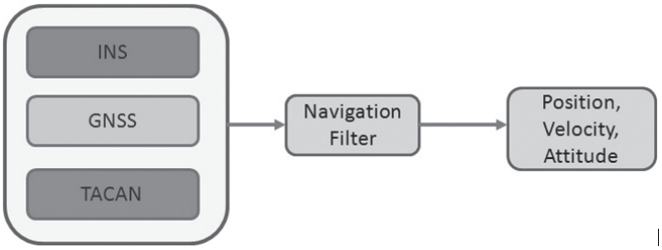

Figure 1. Multi sensor data fusion.

Received 03 September 2012, revised 08 February 2013, online published 23 March 2013

The GNSS receiver simulation requires input from GNSS constellation as GNSS receiver characteristic is dependent on satellites position, inclination and distance from the receiver. GPS almanac data is used to calculate approximate position of satellites in the orbit. The almanac data is downloaded from the US coast guard navigation centre[13]. Ephemeries error model is used from reference[14]. Satellite's position and velocity are computed from equations defined in Appendix II. GNSS Receiver's position and velocity calculations are also described in Appendix II.

The mathematical model for TACAN and VOR/DME is same. Only, the error characteristics for TACAN and VOR/DME are different. TACAN range and bearing models are defined in Appendix III. Sigma error calculation is defind in Appendix IV

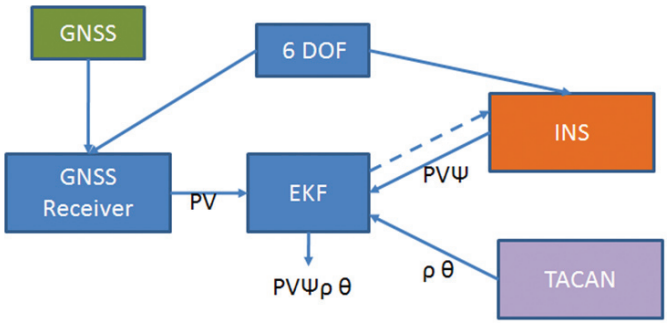

Figure 2. GNSS, INS and TACAN EKF fusion block diagram.

3 NAVIGATION FILTER

The integration of navigation sensors is achieved through navigation filters such as KF, EKF and UKF15. The EKF model is based on measurement compensation. The measurement matrix z is a difference between INS and GNSS measurements. Matrix z is used to correct the INS solutions.

The EKF navigation solution requires system model and measurement model[15]. EKF is used to describe the system which has non linear states. In loose integration there is no interaction between the INS, GNSS and TACAN states therefore the system, transition and system noise covariance matrices may be partitioned as described by Eqs. (1) to (17)[16]

$$x_{system}\begin{bmatrix} Position \\ Volocity \\ Attitude \\ Bias\ Acc \\ Bias\ Gyro \\ TACAN\ RANGE \\ TACAN\ Azimuth \end{bmatrix}_{17\times1} \tag{1}$$

where

$$Position = \begin{bmatrix} x \\ y \\ z \end{bmatrix}_{3\times1} \tag{2}$$

$$Velocity = \begin{bmatrix} V_N \\ V_E \\ V_D \end{bmatrix}_{3\times1} \tag{3}$$

$$Attitude = \begin{bmatrix} \phi \\ \theta \\ \psi \end{bmatrix}_{3\times1} \tag{4}$$

$$Bias\ Acc = \begin{bmatrix} \alpha_x \\ \alpha_y \\ \alpha_z \end{bmatrix}_{3\times1} \tag{5}$$

$$Bias\ Gyro = \begin{bmatrix} g_x \\ g_x \\ g_x \end{bmatrix}_{3\times1} \tag{6}$$

$$TACAN\ RANGE = [\rho]_{1\times1} \tag{7}$$

$$TACAN\ Azimuth = [\theta]_{1\times1} \tag{8}$$

The linearised dynamic model of continuous state space model for dynamics of INS, GNSS and TACAN. is expressed by Eqn. (9).

where

$$F^{n}_{System} = \begin{bmatrix} F_{11} & I_3 & Z_3 & Z_3 & Z_3 & Z_{32} \\ F_{11} & F_{22} & F_{23} & Z_3 & Z_3 & Z_{32} \\ Z_3 & Z_3 & F_{33} & Z_3 & F_{35} & Z_{32} \\ Z_3 & Z_3 & Z_3 & F_{44} & Z_3 & Z_{32} \\ Z_3 & Z_3 & Z_3 & Z_3 & F_{55} & Z_{32} \\ Z_{23} & Z_{23} & Z_{23} & Z_{23} & Z_{23} & F_{66} \end{bmatrix} \tag{9}$$

$$Z_3 = \begin{bmatrix} 0 & 0 & 0 \\ 0 & 0 & 0 \\ 0 & 0 & 0 \end{bmatrix} \tag{10}$$

$$I_3 = \begin{bmatrix} 1 & 0 & 0 \\ 0 & 1 & 0 \\ 0 & 0 & 1 \end{bmatrix} \tag{11}$$

$$Z_{23} = \begin{bmatrix} 0 & 0 & 0 \\ 0 & 0 & 0 \end{bmatrix} \tag{12}$$

$$Z_{32} = \begin{bmatrix} 0 & 0 \\ 0 & 0 \\ 0 & 0 \end{bmatrix} \tag{13}$$

$$F_{66} = \begin{bmatrix} 0 & 0 \\ 0 & 0 \end{bmatrix} \tag{14}$$

Details of F_{11}, F_{12}, F_{22}, F_{33}, F_{35}, F_{44} and F_{55} are in[17]. These are derived from equations described in Appendix I for position, velocity and attitude computation of INS.

The system noise covariance matrix Q is defined by Eqn. (15).

$$Q_{System} = \begin{bmatrix} Z_3 & Z_3 & Z_3 & Z_3 & Z_3 & Z_{32} \\ I_3 & n_{ra}^2 I_3 & Z_3 & Z_3 & Z_3 & Z_{32} \\ Z_3 & I_3 & n_{rg}^2 I_3 & Z_3 & Z_3 & Z_{32} \\ Z_3 & Z_3 & I_3 & n_{bad}^2 I_3 & Z_3 & Z_{32} \\ Z_3 & Z_3 & Z_3 & I_3 & n_{bgd}^2 I_3 & Z_{32} \\ Z_{23} & Z_{23} & Z_{23} & Z_{23} & Z_{23} & Q_{66} \end{bmatrix} \quad (15)$$

where n^2_{ra}, n^2_{rg}, n^2_{bad} and n^2_{bgd} are the power spectral densities (PSD) of the accelerometer random noise, gyros random noise, accelerometer bias variation and gyro bias variation respectively defined[17]. It is assumed that all the three accelerometer and gyros used for INS simulation have same PSD. It is assumed that TACAN range and bearing are linearly dependent. Therefore the derivative of TACAN states are zero. Q_{66} is defined by Eqn.(16).

$$Q_{66} = \begin{bmatrix} TACAN_{RANGE\ Errpr}\,2 & 0 \\ 0 & TACAN_{RANGE\ Errpr}\,2 \end{bmatrix} \quad (16)$$

The measurement matrix is defined by Eqn. (17).

$$H = \begin{bmatrix} 1 & 0 & 0 & 0 & 0 & 0 & 0 & .. & 0 \\ 0 & 1 & 0 & 0 & 0 & 0 & 0 & .. & 0 \\ 0 & 0 & 1 & 0 & 0 & 0 & 0 & .. & 0 \\ 0 & 0 & 0 & 1 & 0 & 0 & 0 & .. & 0 \\ 0 & 0 & 0 & 0 & 1 & 0 & 0 & .. & 0 \\ 0 & 0 & 0 & 0 & 0 & 1 & 0 & .. & 0 \end{bmatrix}_{6\times 17} \quad (17)$$

The statistical nature of INS, GNSS and TACAN are different. Therefore, errors are separated by EKF. The estimated INS error is subsequently subtracted from the INS output.

4. SENSORS SIMULATION AND INTEGRATION

Performance of all sensors is based on input from aircraft dynamic model (ADM)[18].

4.1 INS Simulation

Characteristics which are assumed for accelerometers and gyros for the simulation of INS are tabulated in Table 1.

Sigma errors are tabulated in Table 2 for an update rate of 50 Hz for attitude, velocity and position using ADM as input.

INS attitude, velocity and position are computated without vertical channel correction and do not meet the RNP.

Table 1. INS input characteristic for simulation[20].

Parameters	Value
Earth's angular rate	0.004178074132240 $\frac{rad}{s}$
Accelerometer bias	4.2 μg
Accelerometer scale factor	21 *ppm*
Random walk (accelerometer)	4.2 $\frac{\mu g}{\sqrt{Hz}}$
Gyros bias	0.00084 $\frac{\deg}{h}$
Gyros scale factor	1.67 *ppm*
Random walk (gyros)	.03 $\frac{\frac{\deg}{h}}{\sqrt{Hz}}$

4.2 GNSS Simulation

The YUMA almanac data[14] is downloaded on 06 august 2011 and is used for GPS constellation simulations. The GPS satellites constellation simulation (visibility) is verified at longitude 0.6267° W, latitude 52.0703° N and geodetic height 139 m at 8 hrs, 27 min and 54 s on 7/08/2011 online[19]. The program is written to track the 32 satellites and can be easily modified to track more satellites in future. The program can be easily modified to simulate the GLONASS orbit.

The intermediate parameters require for satellite position calculation is performed for satellite number 3 (PRN 3) and data is taken from YUMA almanac file[14]. Table 4 lists the input parameters require for calculation of satellite coordinates. Similar calculation is performed for the remaining satellites.

The output generated from the Matlab program for calculating the satellite position in ECEF (WGS 84) coordinates is listed in Table 5. For details of terms used, refer[20].

Fig. 3 shows the orbits of all GPS saltellites (31 number). Axes measurements are in meters (ECEF).

4.3 GPS Receiver Simulation

Table 6 shows the position and velocity sigma error of the GPS receiver. DOP factor of less than 2.5 is considered for 4 best DOPs.

Table 2. Velocity, position, attitude sigma error

Measurements	Values (m/s)	Measurements	Values (m)	Measurements	Values (degree)
$\sigma_{Velocity\ North}$	8.18	$\sigma_{Position\ North}$	1693.04	σ_{roll}	0.7223
$\sigma_{Velocity\ East}$	0.86	$\sigma_{Position\ East}$	182.90	σ_{pitch}	0.0541
$\sigma_{Velocity\ yaw}$	3.51	$\sigma_{Position\ yaw}$	93.05	σ_{yaw}	0.6787
σ_{Total}	8.94	$\sigma_{Position\ Total}$	1705.43	σ_{Total}	0.9926

Table 3. Values used for satellite coordinate calculation[20]

Terms	values	Units	Terms	values	Units
μ	3.986005 x 10^{14}	$\frac{m^2}{s^2}$	C_{rs}	7.321875 x 10^{1}	m
Ω_e	7.292115167 x 10^{-5}	$\frac{rad}{s}$	C_{ic}	6.146729 x 10^{-8}	rad
c	2.99792458 x 10^{8}	$\frac{m}{s}$	C_{is}	2.086163 x 10^{-7}	Rad
C_{uc}	4.017726 x 10^{6}	rad	Δ n	1.45853639 x 10^{-4}	$\frac{Semicircle}{s}$
C_{us}	7.698312 x 10^{-6}	rad	$IDOT$	9.178953 x 10^{-11}	$\frac{Semicircle}{s}$
C_{rc}	2.259375 x 10^{2}	m	$Af2$	0.00000	$\frac{s^2}{s^2}$

Table 4. YUMA Alamac data for PRN 03

Terms	Values	Units	Terms	Values	Units
M_0	-0.2194783688 x 10^{0}	*Semicircle*	ω	1.116163492	*Semicircle*
E	0.2794265747 x 10-^{2}	*Dimensionless*	$\overset{0}{\Omega}$	-0.8145434549E-008	$\frac{Semicircle}{s}$
$\sqrt{a}$	5153.604980	$m^{\frac{1}{2}}$	$t_{0\varepsilon}$	61440.0000	s
Ω_0	0.2861869574E+001	*Semicircle*	$Af0$	-0.7629394531 x 10-^{5}	s
i_0	0.9296073914°	*Semicircle*	$Af1$	0.3637978807E-011	$\frac{s}{s}$

Table 5. GPS satellite position (PRN 03)

Terms	Values	Terms	Values
α	26835551.59417703400	δi_3	-0.00000011339
n_o	0.00014361610	μ_3	-1.43984826165
t_3	0.00075217704	r_3	26841562.97797437400
n	0.00028946974	i_3	0.92962446853
M_3	53.99297081061	x'_3	3504814.25677414750
f_3	-2.55600587966	y'_3	-26611760.18466417100
E_3	2.55585142583	Ω_3	-15.27674487674
ϕ_3	-1.43984238766	x_3	-9837106.36624007300
$\delta\mu_3$	-0.00000587399	y_3	12995363.14535391300
δr_3	-237.19060061759	z_3	-21326541.63619175900

Table 6. Position, velocity sigma error

Measurements	Values (m)	Measurements	Values ($\frac{m}{s}$)
$\sigma_{position_{xECEF}}$	**1.1073**	$\sigma_{velocity_x}$	**1.5741**
$\sigma_{position_{yECEF}}$	**2.9747**	$\sigma_{velocity_y}$	**1.1877**
$\sigma_{position_{zECEF}}$	**2.3385**	$\sigma_{velocity_z}$	**0.70150**
$\sigma_{position_{Total}}$	**3.9425**	$\sigma_{velocity_{Total}}$	**2.0930**

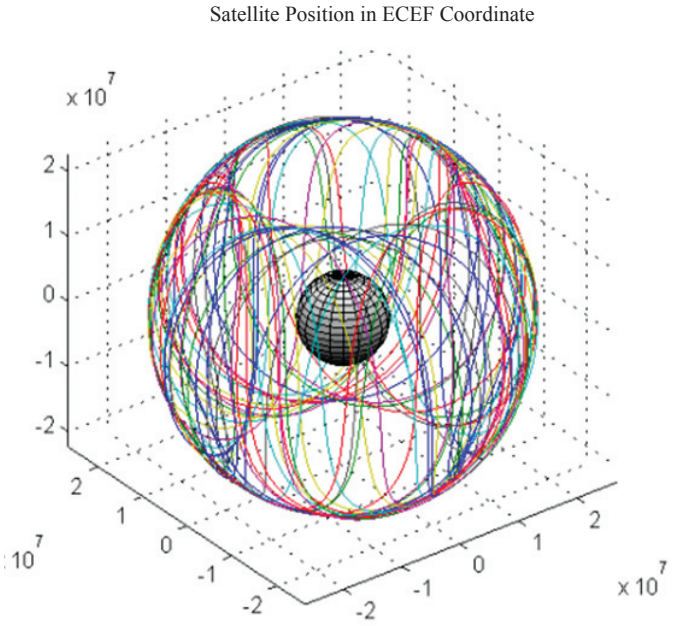

Figure 3. GPS Satellites trace for one orbital period.

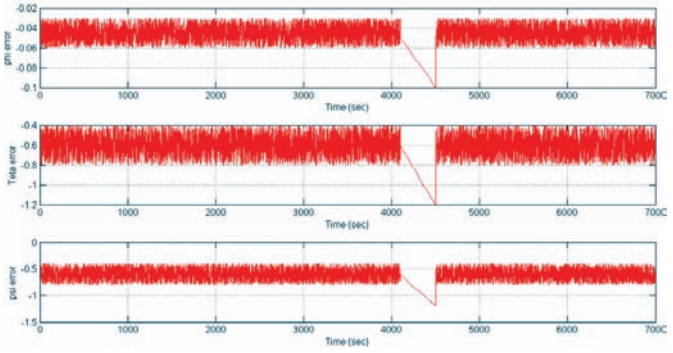

Figure 4. Attitude solution with filter.

4.4 TACAN Simulation

Typical TACAN range error and azimuth error are assumed as meters and respectively. In this analysis, TACAN ground station location is assumed as 519 m North, 153 m East and 5 m down in NED frame. Simulation result of range and bearing are shown in Figs. 5 and 6 as actual TACAN range and bearing index respectively.

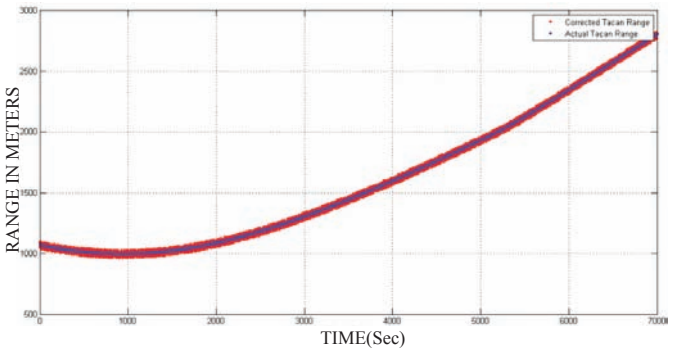

Figure 5. TACAN range solution.

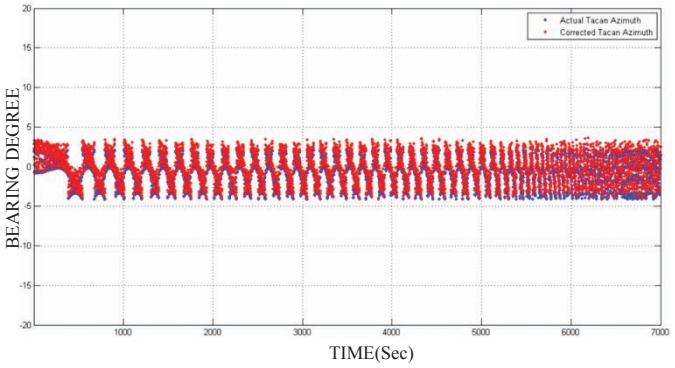

Figure 6. TACAN bearing solution.

4.5 EKF Simulation Results for INS, GNSS and EKF

GNSS position solution is converted into NED frame. Update rate of EKF filter is 1 Hz and INS update rate is 50 Hz. GNSS and TACAN update rate is 1 Hz. INS, GNSS and TACAN simulation parameters are same as used in section 4.1, 4.2, 4.3 and 4.4.

Fig. 4 shows the attitude solution obtained from the EKF filter of INS, GNSS and TACAN. In this solution GNSS signal is temporarily unavailable from 4100 s to 4500 s. During this period the solution accumulates the similar errors as of standalone INS. Similar analysis is performed for velocity and position. attitude, velocity and position sigma errors are tabulated in Table 7.

The sigma error is better than the standalone INS solutions.

TACAN range and bearing filter solutions are shown in Figs. 5 and 6 respectively.

Table 7. Attitude, velocity and position sigma error with filter

Measurements	Values (degree)	Measurements	Values $(\frac{m}{s})$	Measurements	Values (m)
$\sigma_{roll\ EKF}$	0.6067	$\sigma_{velocity\ North\ EKF}$	1.6369	$\sigma_{positional\ North\ EKF}$	3.7745
$\sigma_{pitch\ EKF}$	0.0441	$\sigma_{velocity\ East\ EKF}$	1.1848	$\sigma_{position\ East\ EKF}$	4.1973
$\sigma_{yaw\ EKF}$	0.6157	$\sigma_{velocity\ Down\ EKF}$	0.9289	$\sigma_{position\ Down\ EKF}$	3.4662
$\sigma_{Total\ EKF}$	0.8657	$\sigma_{velocity\ Total\ EKF}$	2.2240	$\sigma_{position\ Total\ EKF}$	6.6241

5 CONCLUSION

The loose integration of INS, GNSS and TACAN is performed using EKF. The data link may be added to the same navigation filter to provide the navigational fix in terms of position and velocity from cooperating platforms. The error budget of the platform can be computed based on sigma error of the cooperating platforms with different sensors accuracies and sigma errors. This will pave the way for development of decision support tool for flight operations.

REFERENCES

1. Gustavsson, P. Development of a Matlab bassed GPS constellation simulation for navigation algorithm developments. University of Technology, Lulea, 2005, Master Thesis.
2. Kelly, R.J. & Davis, J.M. Requires navigation performance for precision approach and landing with GNSS application. *J. Institute Navigation*, 1994, **41**(1), 1-30.
3. Eurocontrol.http://www.eurocontrol.int/eatm/gallery/content/public/library/euro_stds/Eng/rnav/RNAV_Standard_Ed_22a_web.pdf [Accessed on 30/08/2012]
4. Allerton, D. & Jia, H. A review of multisensor fusion. *Journal Navigation*, 2005, **58**, 405-417.
5. Seraji, H. & Serrano, N. A multisensor decision fusion system for terrain safety assessment. *IEEE Trans. Robatics*, 2009, **25**(1), 98-108.
6. Babu, R. & Wang J. Ultra tightly GPS/INS/PL integeration: Kalman filter performance analysis. *GPS Solut.*, 2009, **13**(1), 75-82.
7. Wang J. & Liang, K. Multi sensor data fusion based on fault detection and feedback for integerated navigation systems. *In* the International symposium on integrated information technology application workshops, Beijing, IEEE Computer Society, 21-22 Dec 2008. pp. 232-35.
8. Lemay, L.; Chu, C.C & Egziabher, G.D. Precise input and output error characterization for loosely integerated INS/GPS/Camers navigation system. *In* the proceedings of the national technical meeting; Institute of navigation, San Diego, California, 2011. **2**, pp. 880-894.
9. Lijun, W.; Huichang, Z. & Xiaoniu, Y. The modeling and simulation for GPS/INS integerated navigation system. *In* the ICMMT 2008 proceedings, IEEE, 2008. Nanjing, China, 21-24 April 2008, pp. 1991-994.
10. Celestial Observer. http://www.calsky.com/ [Accessed on 06/08/2011].
11. Edward, L.W.; Clark, J.B. & Bevly, D.M. Implementation details of a deeply integerated GPS/INS software receiver. *In* Position Location and Navigation Symposium (PLANS), 2010, IEEE/ION, 4-6 May 2010, pp. 1137-146.
12. Han, L.J. & Wei, M. Adaptive EKF filter based on genetic algorithm for tightly coupled integrated inertial and GPS navigation. *In* the 2nd International conference on Intelligent computing technology and automation, 2009. Changsha, Hunan, 10-11 Oct 2009, **1**, pp. 520-524.
13. U.S Cost Guard Navigation Centre http://www.navcen.uscg.gov/?pageName=gpsAlmanacs [Accessed on 06/08/2011]
14. Joerger, M.; Neale, J.; Pervan, B. & Datta, B.S. Measurement error models and fault detection algorithms for multi constelation navigation systems. *In* Position Location and Navigation Symposium (PLANS), 2010 IEEE/ION, Indian Wells, USA, 4-6 May 2010, pp. 927-946.
15. Zarchan P. & Howard M. Fundamental of Kalman filtering : A practical approach. Ed 3rd, AIAA, 2005 765p.
16. Shankar. R. Development of multi-sensor navigation system using on-board sensor resources. Cranfield University, U.K, April 2011. (MSc, Thesis).
17. Paul, D.G. Principles of GNSS, inertial and multisensor integrated navigation systems. Artech house, London, 2008.
18. Aerosond UAV. http://www.aerosonde.com/ [Accessed on 15/08/2011].
19. Celestial Observer. http://www.calsky.com/ [Accessed on 06/08/2011].
20. Mohinde, S.G.; Lawrence, R.W. & Angus, P.A. Global positioning systems, inertial navigation. Ed 2nd, 2007, A John Wiley & Sons Inc. 517 p.
21. Titterton, D.H. & Weston, L.J. Strapdown inertial navigation technology. Institution of Electrical Engineers. Ed 2nd, 2005, 549p.
22. Robert, M.R. Applied mathematics in integrated navigation systems. AIAA. Ed 3rd, 2007, 340p.
23. Piotr, K. Integration of INS with TACAN and Altimeter. Military university of technology, 2 Gen. S. Kaliski, Poland, 2007.

Contributor

Mr Ravi Shankar has received BSc(Eng) (Comp. Sc. Eng.) from B.I.T Sindri, Jharkand and MSc (Aerospace Vehicle Design (Avionics)) from Cranfield University, U.K., in 2002 and 2011 respectively. He is presently working at Hindustan Aeronautics Limited, Banglore. He worked in the area of development of controller for ground based radio, GPS receiver, ground-based voice recorder, VoIP integration, communication system integration and testing on military aircraft. Presently working on control software development for software defined radio.

APPENDIX I[21]

Gyros are generalised in mathematical from as described by the Eqn. (18).

$$\omega_{out} = \omega_{in} + \Delta_B + \Delta_R + \Delta_{SF}\omega_{in} \tag{18}$$

where ω_{out} and ω_{in} are the gyro output and input respectively, Δ_B is the gyro bias, Δ_R is the gyro random drift rate, Δ_{SF} is the gyro scale factor.

Accelerometers are generalised in mathematical from as described by the Eqn. (19).

$$f_{out} = f_{in} + \varepsilon_B + \varepsilon_R + \Delta_{SF} f_{in} \tag{19}$$

where f_{out} and f_{in} are the output and input of an accelerometer, ε_B is the accelerometer bias, ε_R is an accelerometer time dependent random bias. Δ_{SF} is the accelerometer scale factor error.

Quaternion differential equation (attitude) in NED frame is defined by Eqn. (20).

$$\frac{d}{dt}\begin{bmatrix} q_0 \\ q_1 \\ q_2 \\ q_3 \end{bmatrix} = 0.5 * \begin{bmatrix} 0 & -\omega^b_{n/b,x} & -\omega^b_{n/b,y} & -\omega^b_{n/b,z} \\ \omega^b_{n/b,x} & 0 & \omega^b_{n/b,z} & -\omega^b_{n/b,y} \\ \omega^b_{n/b,y} & -\omega^b_{n/b,z} & 0 & \omega^b_{n/b,x} \\ -\omega^b_{n/b,z} & \omega^b_{n/b,y} & -\omega^b_{n/b,x} & 0 \end{bmatrix} + \begin{bmatrix} q_0 \\ q_1 \\ q_2 \\ q_3 \end{bmatrix} \tag{20}$$

Velocity equation is defined by Eqn.(21).

$$\Delta v^n = C^n_b(t_i)[\Delta v^b + \Delta\theta \times \Delta v^b] \tag{21}$$

The position is expressed by direction cosine matrix differential Eqn. (22)

$$C^n_e = -\Omega^n_{e/n} C^n_e \tag{22}$$

Attitude Error Equations is defined by Eqn. (23)

$$\delta C^n_b = -(\phi\times) C^n_b \tag{23}$$

Velocity error equation with respect to velocity and earth radius yields is defined by Eqn. (24)

$$\delta\omega^n_{e/n} \approx \begin{bmatrix} -\frac{\delta v^n_y}{R} - \frac{\rho_x}{R}\delta h \\ -\frac{\delta v^n_x}{R} - \frac{\rho_y}{R}\delta h \\ \delta\rho_z \end{bmatrix} \tag{24}$$

Position error equations is defined as

$$\delta\dot{\theta} = \delta\rho - \omega^n_{e/n} \times \delta\theta \tag{25}$$

The single DCM result from the rotation of Φ about x axis, θ about y axis and ψ about z axis is defined by Eqn. (26).

$$C^j_i = \begin{bmatrix} 1 & 0 & 0 \\ 0 & \cos(\Phi) & \sin(\Phi) \\ 0 & -\sin(\Phi) & \cos(\Phi) \end{bmatrix}\begin{bmatrix} \cos(\theta) & 0 & -\sin(\theta) \\ 0 & 1 & 0 \\ \sin(\theta) & 0 & \cos(\theta) \end{bmatrix}\begin{bmatrix} \cos(\psi) & \sin(\psi) & 0 \\ -\sin(\psi) & \cos(\psi) & 0 \\ 0 & 0 & 1 \end{bmatrix} =$$

$$\begin{bmatrix} \cos(\theta)*\cos(\psi) & -\cos(\theta)*\sin(\psi) & \sin(\Phi)*\sin(\psi) \\ & +\sin(\Phi)*\sin(\theta)*\cos(\psi) & +\cos(\Phi)*\sin(\theta)*\cos(\psi) \\ \cos(\theta)*\sin(\psi) & \cos(\theta)*\cos(\psi) & -\sin(\Phi)*\cos(\psi) \\ & +\sin(\Phi)*\sin(\theta)*\sin(\psi) & +\cos(\Phi)*\sin(\theta)*\sin(\psi) \\ -\sin(\theta) & \sin(\Phi)*\cos(\theta) & \cos(\Phi)*\cos(\theta) \end{bmatrix} \tag{26}$$

Position in orbital plane is defined by Eqns. (27) and (28), where μ_k and r_k are corrected argument of latitude and radius respectively.

$$x'_k = r_k \cos\mu_k \tag{27}$$

$$y'_k = r_k \sin\mu_k \tag{28}$$

Velocity in orbital plane is defined by Eqns. (29) and (30).

$$\dot{x}'_k = -\sqrt{\frac{\mu}{a(1-e^2)}} * \sin\mu_k \tag{29}$$

$$\dot{y}'_k = -\sqrt{\frac{\mu}{a(1-e^2)}} * [(\cos]\mu_k + e) \tag{30}$$

Position of K^{th} satellite in ECEF coordinate is defined from Eqns. (31) to (33), where i_k is inclination between inclination plan and orbital plan.

$$x_k = x'_k \cos\Omega_k - y'_k \cos i_k \sin\Omega_k \tag{31}$$

$$y_k = x'_k \sin\Omega_k + y'_k \cos i_k \cos\Omega_k \tag{32}$$

$$z_k = y'_k \sin i_k \tag{33}$$

Velocity of K^{th} satellite in ECEF coordinate is defined by Eqns (34) to (36)

$$\dot{x}_k = \dot{x}'_k \cos\Omega_k - \dot{y}'_k \cos i_k \sin\Omega_k \tag{34}$$

$$\dot{y}_k = \dot{x}'_k \sin\Omega_k + \dot{y}'_k \cos i_k \cos\Omega_k \tag{35}$$

$$\dot{z}_k = \dot{y}'_k \sin i_k \tag{36}$$

Pseudo range is computed from Eqn. (37), where *x,y* and *z* are users coordinates and *X, Y* and *Z* are satellite coordinates.

$$\rho\sqrt{(x-X)^2 + (y-Y)^2 + (z-Z)^2} \tag{37}$$

The $\Delta\rho$ matrix is derived from Eqn. (37) and n is the number of visible satellites as defined by Eqn. (38)

$$\Delta\rho = \begin{bmatrix} \rho_1 \\ \rho_2 \\ \rho_3 \\ \cdots \\ \rho_n \end{bmatrix}_{n\times 1} \tag{38}$$

APPENDIX II[20, 22]

$$\Delta X = \begin{bmatrix} \Delta x \\ \Delta y \\ \Delta z \\ \Delta t \end{bmatrix}_{4\times 1} \tag{39}$$

$$H \times \Delta X = \Delta \rho \tag{40}$$

The H matrix is defined by Eq (41).

$$H = \begin{bmatrix} c_{x1} & c_{y1} & c_{z1} & 1 \\ c_{x2} & c_{y2} & c_{z2} & 1 \\ .. & .. & ... & \\ c_{xn} & c_{yn} & c_{zn} & 1 \end{bmatrix}_{n\times 4} \tag{41}$$

Where $c_k=(c_{xk}, c_{yk}, c_{zk})$ is a unit vector from user's location to K^{th} satellite's location

The offset (Δx) is computed by Eqn. (42).

$$\Delta X = (H^T * H)^{-1} H^T * \Delta \tag{42}$$

DOPs are obtained by matrix $(H^T * H)^{-1}$. The term σ_{ij} represents covariance of error in computed position and time whereas user's covariance is assumed as one m^2.

$$(H^T * H)^{-1} = \begin{bmatrix} \sigma_{11} & \sigma_{12} & \sigma_{13} & \sigma_{14} \\ \sigma_{21} & \sigma_{22} & \sigma_{23} & \sigma_{24} \\ \sigma_{31} & \sigma_{32} & \sigma_{33} & \sigma_{34} \\ \sigma_{41} & \sigma_{42} & \sigma_{43} & \sigma_{44} \end{bmatrix} \tag{43}$$

DOPs are defined by Eqs (44) to (48).

$$GDOP = \sqrt{\sigma_{11} + \sigma_{22} + \sigma_{33} + \sigma_{44}} \tag{44}$$

$$PDOP = \sqrt{\sigma_{11} + \sigma_{22} + \sigma_{33}} \tag{45}$$

$$HDOP = \sqrt{\sigma_{11} + \sigma_{22}} \tag{46}$$

$$VDOP = \sqrt{\sigma_{33}} \tag{47}$$

$$TDOP = \sqrt{\sigma_{44}/c} \tag{48}$$

User velocity $\dot{x}, \dot{y}$ and $\dot{z}$ is calculated from Eqn.(49).

$$\begin{bmatrix} -\dot{\rho}_1 + \frac{1}{\rho_1}\left[\dot{X}_1(X_1 - x) + \dot{Y}_1(Y_1 - y) + \dot{Z}_1(Z_1 - z)\right] \\ -\dot{\rho}_2 + \frac{1}{\rho_2}\left[\dot{X}_2(X_2 - x) + \dot{Y}_2(Y_2 - y) + \dot{Z}_2(Z_2 - z)\right] \\ -\dot{\rho}_3 + \frac{1}{\rho_3}\left[\dot{X}_3(X_3 - x) + \dot{Y}_3(Y_3 - y) + \dot{Z}_3(Z_3 - z)\right] \end{bmatrix} = \begin{bmatrix} \frac{X_1 - x}{\rho_1} & \frac{Y_1 - y}{\rho_1} & \frac{Z_1 - z}{\rho_1} \\ \frac{X_2 - x}{\rho_2} & \frac{Y_2 - y}{\rho_2} & \frac{Z_2 - z}{\rho_2} \\ \frac{X_3 - x}{\rho_3} & \frac{Y_3 - y}{\rho_3} & \frac{Z_3 - z}{\rho_3} \end{bmatrix} \begin{bmatrix} \dot{X} \\ \dot{Y} \\ \dot{Z} \end{bmatrix} \tag{49}$$

APPENDIX III

TACAN range and bearing are calculated from Eqn.(50) and Eqn. (51) respectively[23] where (x,y,z) are aircraft position and (X,Y,Z) are TACAN ground station location.

$$\rho_{TACAN} = \sqrt{(x-X)^2 + (y-Y)^2 + (z-Z)^2} + b_{TACAN} + \upsilon_{TACAN} \tag{50}$$

Where b_{TACAN} is a corrupting bias and u_{TACAN} is a measurement noise.

$$\theta = \cos^{-1}\left(\frac{y-Y}{\rho_{TACAN}}\right) \tag{51}$$

APPENDIX IV

Sigma error is defined by Eqn. (52), where N is the number of samples, *measurement* is the measured data and *input* is the expected value.

$$\sigma = \sqrt{\frac{\sum_1^N (measurement - input)^2}{N}} \tag{52}$$